OPEN ACCESS
IOP Publishing
Superconductor Science and Technology
Supercond. Sci. Technol. **33** (2020) 115012 (12pp)
https://doi.org/10.1088/1361-6668/abb590

Pulsed-field magnetisation of Y-Ba-Cu-O bulk superconductors fabricated by the infiltration growth technique

Devendra K Namburi[1], K Takahashi[2], T Hirano[2], T Kamada[2], H Fujishiro[2], Y-H Shi[1], D A Cardwell[1], J H Durrell[1] and M D Ainslie[1]

[1] Department of Engineering, University of Cambridge, Cambridge CB2 1PZ, United Kingdom
[2] Department of Physical Science and Materials Engineering, Faculty of Science and Engineering, Iwate University, 4-3-5 Ueda, Morioka 020-8551, Japan

E-mail: dkn23@cam.ac.uk and ndevendra@gmail.com

Received 19 June 2020, revised 28 July 2020
Accepted for publication 6 September 2020
Published 30 September 2020

Abstract

Bulk high temperature superconductors based on the rare-earth copper oxides can be used effectively as trapped field magnets capable of generating large magnetic fields. The top-seeded infiltration growth (TSIG) processing technique can provide a more homogeneous microstructure and therefore more uniform superconducting properties than samples grown using conventional melt growth processes. In the present investigation, the properties of bulk, single grain superconductors processed by TSIG and magnetised by the pulsed-field magnetisation technique using a copper-wound solenoid have been studied. A trapped field of ~3 T has been achieved in a 2-step buffer-assisted TSIG-processed Y-Ba-Cu-O (YBCO) sample at 40 K by magnetising the bulk superconductor completely via a single-pulse magnetisation process. Samples were also subjected to pulsed-field magnetisation at 65 K and by conventional field-cooled magnetisation at 77 K for comparison. Good correlation was observed between the microstructures, critical current densities and trapped field performance of bulk samples fabricated by TSIG and magnetised by pulsed-field and field-cooled magnetisation. The homogeneous distribution of Y_2BaCuO_5 inclusions within the microstructure of bulk YBCO samples fabricated by the 2-step buffer-assisted TSIG process reduces inhomogeneous flux penetration into the interior of the sample. This, in turn, results in a lower temperature rise of the bulk superconductor during the pulsed-field magnetisation process and a more effective and reliable magnetisation process.

Keywords: pulsed-field magnetisation, bulk YBCO, infiltration and growth, trapped field, homogeneous and dense microstructure, flux-pinning strength

(Some figures may appear in colour only in the online journal)

1. Introduction

Bulk, (RE)-Ba-Cu-O ((RE)BCO, where RE = rare earth or Y) high temperature superconductors fabricated in the form of large, single grains can be used to form strong trapped field magnets and hence have considerable potential for a wide variety of engineering and technological applications, including, but not limited to, magnetic resonance imaging,

magnetic separation, rotating machines and non-contact mixers [1–4]. Bulk superconductors are unique in that their magnetisation scales with the size (diameter) of the single grain, unlike conventional Sm-Co or Nd-Fe-B permanent magnets whose magnetisation is generally independent of sample volume. Hence, the larger the size of the (RE)BCO bulk single grain and the higher its current-carrying ability, the larger its trapped magnetic field. Examples of the trapped field potential of bulk (RE)BCO superconductors include 14.3 T in conventional undoped YBCO [5], 16 T in YBCO processed with Ag and Zn [6], 17.24 T at 29 K in YBCO reinforced with resin impregnation and Wood's metal [7] and 17.6 T at 26 K in GdBCO with Ag, reinforced with shrink-fit stainless steel [8] in a two-sample stack configuration.

The substantial effort world-wide made over the last 30 years to refine various melt-process fabrication techniques has established effective pathways and processes for growing large (RE)BCO single grains with engineered microstructures that exhibit superior superconducting and field generating properties [6–12]. However, inherent limitations to a number of these processes, such as considerable sample shrinkage during processing [13, 14] and non-uniform superconducting properties across the sample volume [15], have motivated researchers to seek alternative approaches to sample fabrication. In this context, the infiltration and growth technique [13, 14, 16–22] has emerged as a competitive alternative to top seeded melt growth (TSMG), in particular. The infiltration and growth technique has, however, two significant drawbacks: (i) the success rate of single grain growth has, to-date, been very poor, due primarily to the presence of a relatively large component of aggressive liquid phase during the melt process, which makes the crystallisation and growth steps particularly challenging, and (ii) the superconducting properties of samples fabricated by this approach have been characteristically inferior compared to those fabricated by conventional melt-growth processes. Only recently have significant improvements been made towards developing a more effective infiltration and growth process, which have led to a significant enhancement in the reliability of (RE)BCO single grain growth and improved superconducting properties [23–26]. Three particularly significant developments made in the area of infiltration and growth processing are: (i) a suitable liquid-phase reservoir pellet (of appropriate composition, size and weight), (ii) integration of a buffer technique to aid the seeding process, and (iii) tuning and control of the RE_2BaCuO_5 (RE-211) distribution within the microstructure to facilitate improved flux pinning. The combination of these three enhancements has led to the development of the so-called 2-step buffer-assisted top-seeded infiltration and growth processing methodology, which has enabled the fabrication of (RE)BCO bulk superconductors with superior and uniform superconducting properties, with critical current densities (J_cs) exceeding 50 000 A cm^{-2} at 77 K [27].

Magnetisation is an important process in developing effective engineering applications of (RE)BCO bulk superconductors, of which field cooled magnetisation (FCM) and pulsed-field magnetisation (PFM) are two effective approaches for this purpose. Although FCM allows higher trapped fields to be generated, it requires access to a large magnetising field, provided usually by a large and expensive superconducting magnet. This is not feasible for many practical applications, however, where *in-situ* charging is a necessity (for example, for rotating machines). It is, however, an extremely useful technique to characterise the maximum trapped field capability of a given bulk sample or system. The alternative PFM approach, on the other hand, is quick, compact and relatively inexpensive and is therefore considered generally to be the most practical magnetisation method for engineering applications. PFM is performed by applying a magnetic field, typically of duration of the order of 100s of milliseconds, using either a solenoid, vortex or split coil configuration [28, 29]. One significant disadvantage of PFM is the considerable temperature rise during the process associated with the rapid dynamic movement of magnetic flux within the superconductor, although even this, if addressed appropriately, can facilitate the trapping of significant magnetic fields for engineering applications of bulk single grains [28]. Recently, several modifications and significant improvements have been made to the PFM approach by optimising the pulse rise time, pulse duration, efficient cooling and heat dissipation and so on, which have improved the efficiency and reliability of PFM [30–32]. Homogeneity of J_c plays a critical role in the magnetic flux dynamics during PFM and any inhomogeneities within the bulk can result in localised heating, a larger temperature rise and a reduced and/or distorted trapped field profile [30]. We are not aware of any PFM studies to date on bulk samples fabricated by infiltration and growth processing that are motivated by the positive impact anticipated from a more homogeneous microstructure, which is the focus of the current investigation. Furthermore, this work examines pathways to improve the trapped field ability of single grains using PFM based specifically on the crystal growth technique, rather than more generally on obtaining higher and uniform J_c characteristics.

In this work, detailed PFM studies have been carried out on two bulk single grain YBCO samples fabricated by infiltration growth techniques. One of these samples was fabricated via conventional top-seeded infiltration growth (TSIG) processing, but using a liquid phase reservoir of optimised composition, and the other by the recently developed, so-called, '2-step BA-TSIG' approach. Both these fabrication techniques exploit the use of a buffer pellet. PFM was carried out at 65 K and 40 K using a solenoid coil with applied fields of up to 6 T for both samples. Additionally, FCM measurements were used to assess the trapped field capability of the samples at 77 K, and J_c and $J_c(B)$ of small sub-specimens cut from each bulk single grain were measured at several temperatures to assess the strength and uniformity of the intrinsic flux pinning. Finally, microstructural studies were performed to understand the correlation between the Y_2BaCuO_5 (Y-211) content present in the continuous $YBa_2Cu_3O_{7-x}$ (Y-123) phase matrix and the observed superconducting properties of the single grain.

Table 1. Dimensions of the TSIG-processed YBCO samples investigated in this study.

Sample	YBCO	YBCO
Sample code	#700	#911
Fabrication route	1-step Buffer-assisted TSIG	2-step Buffer-assisted TSIG
Diameter of the preform compact	31.3 mm	32.0 mm
Diameter of the sample, as grown	30.8 mm	32.5 mm
Diameter of the sample, after machining	29.5 mm	29.1 mm
Thickness of the sample, after machining	16.4 mm	14.1 mm
316-Stainless-steel ring: Inner diameter	29.52 mm	29.12 mm
316-Stainless-steel ring: Outer diameter	56 mm	56 mm

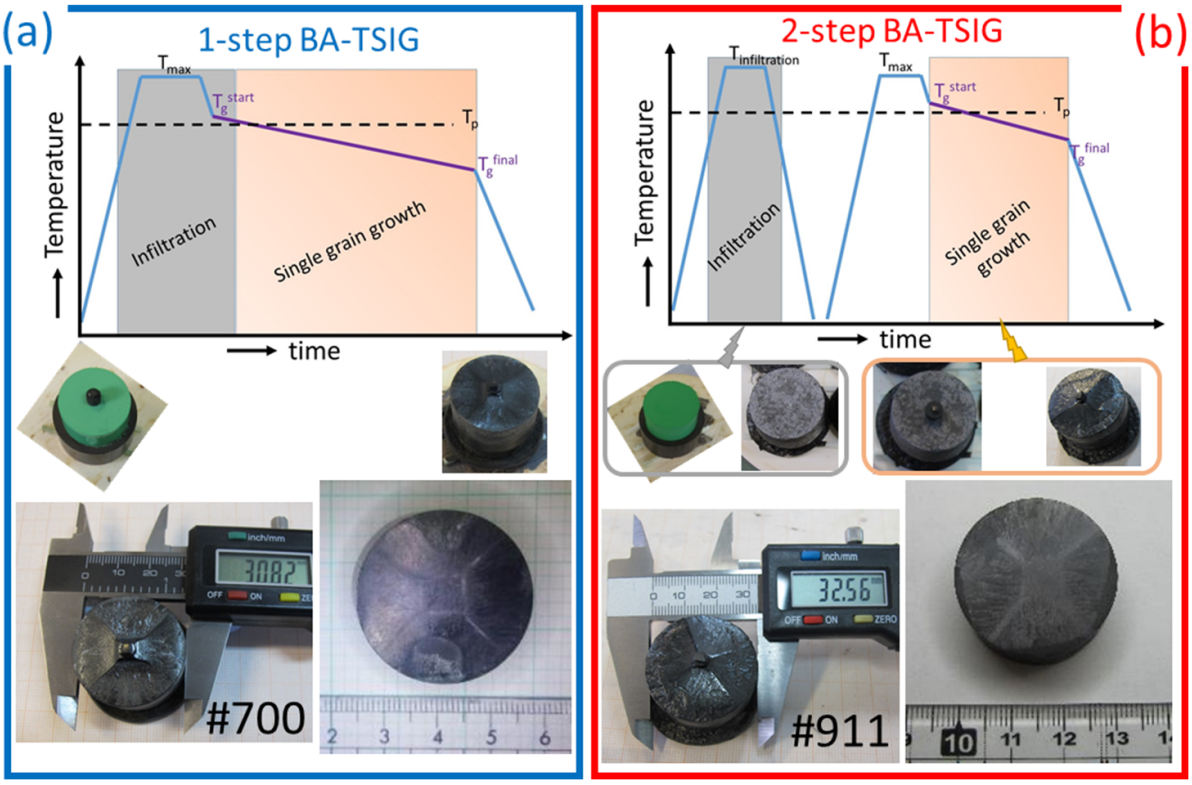

Figure 1. YBCO samples fabricated via (a) 1-step BA-TSIG and (b) 2-step BA-TSIG techniques. The heat treatments for each fabrication approach are shown in the figure. T_{max}, T_p, T_g^{start} and T_g^{final} represent the maximum processing temperature, peritectic temperature, growth-starting temperature and growth-final temperatures of the respective processes. The fully processed, YBCO single grains obtained after heat treatment (labelled as #700 and #911) are also shown, including both the machined and polished surfaces of the samples.

2. Sample fabrication and characterisation

2.1. TSIG-processed YBCO

Two YBCO samples were fabricated for this study; one via conventional buffer-assisted top-seeded infiltration and growth (hereafter referred to as '1-step BA-TSIG') and the other via the 2-step BA-TSIG technique developed recently. The dimensions of both samples were ~30 mm in diameter and ~15 mm in height. Additional details on the sample dimensions are provided in table 1. Schematic diagrams illustrating the detail of the heat treatments for these two fabrication methodologies and with photographs of the samples produced, are shown in figures 1(a) and (b), respectively.

The precursor sample assembly for fabricating YBCO single grains by the infiltration growth-based techniques investigated here consisted of a primary pre-form compact comprised of Y-211 + 1 wt.% CeO_2 placed in direct contact with a liquid phase reservoir pellet, comprised of a mixture of Yb_2O_3, $BaCuO_2$, and CuO in the ratio 1: 10: 6 [33, 34], with each assembly supported by a thin disc of Yb_2O_3. A buffer pellet of composition 75 wt.% Y-123 + 25 wt.% Y-211 and 5 mm in diameter was placed on the pre-form and capped with an NdBCO seed crystal to promote heterogeneous nucleation and subsequent single grain growth. The buffer-aided growth technique was used both to overcome diffusion of the seed crystal element into the bulk sample at elevated temperature and, simultaneously, to minimise liquid phase segregation in

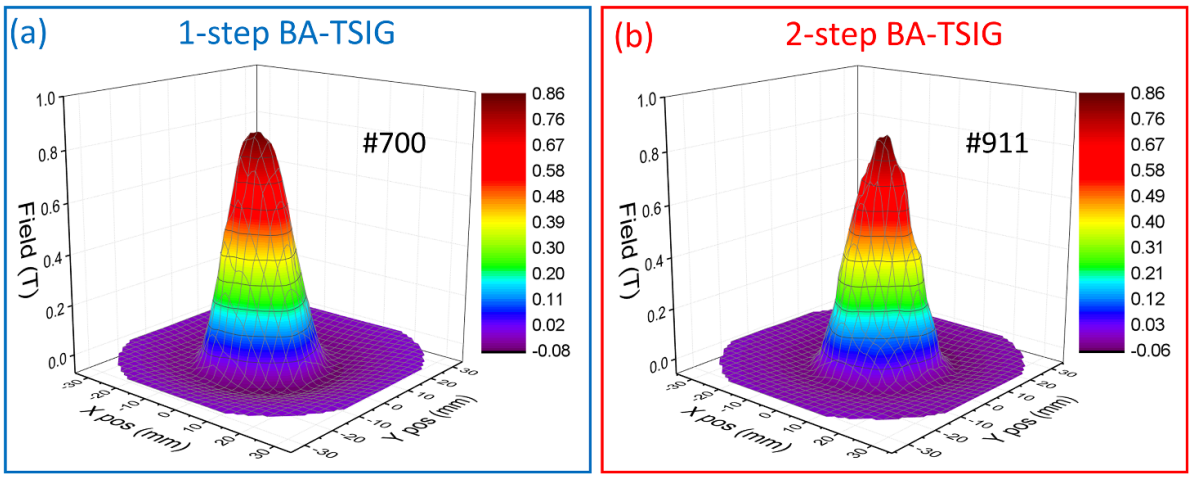

Figure 2. (a) and (b) show trapped field profiles measured at 77 K after field-cooled magnetisation using a 1.4 T electromagnet for the TSIG-processed YBCO samples #700 and #911 at heights of 1.5 mm and 2 mm, respectively, above the top surface of the single grain.

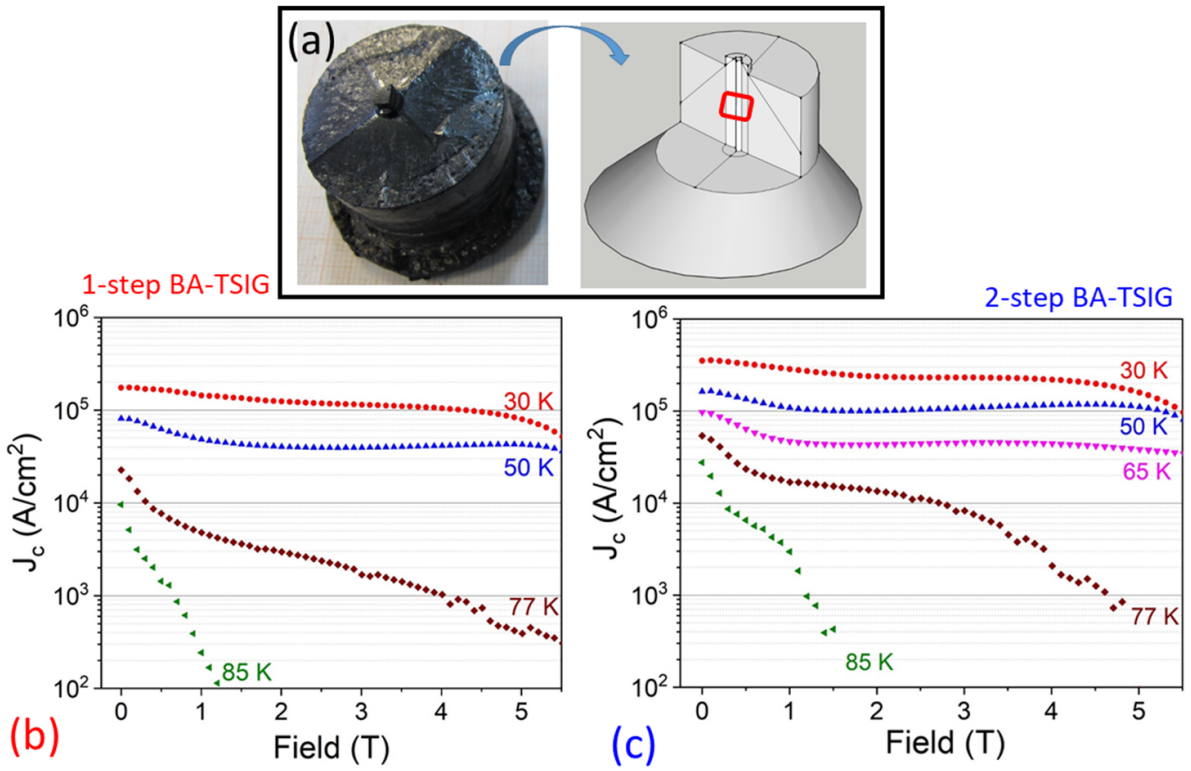

Figure 3. (a) Location within the parent single grain (central region, highlighted by the red box) of the sub-specimens extracted for comparative magnetic measurements. Field dependence of the critical current density, $J_c(B)$, obtained at different temperatures between 30–85 K for (b) 1-step BA-TSIG and (c) 2-step BA-TSIG processing techniques.

the vicinity of the seed crystal, thereby minimising the probability of seed failure during processing [35]. Further details of each of these fabrication methodologies can be found elsewhere [23, 27]. The single-grain YBCO samples fabricated by the 1-step and 2-step BA-TSIG techniques were subsequently oxygenated at a temperature of 450 °C for 200 h in flowing oxygen (with a flow rate of 100 ml min^{-1}) to transform the non-superconducting tetragonal phase into the orthorhombic superconducting phase. The trapped field capability of the samples at 77 K was then measured following field-cooled magnetisation.

2.2. *Trapped field measured via field-cooled magnetisation*

The surfaces of each single grain were polished flat prior to field-cooling in liquid nitrogen in an applied magnetic field, generated by an electromagnet, of 1.4 T. The external field was removed once the field-cooled sample had reached thermal

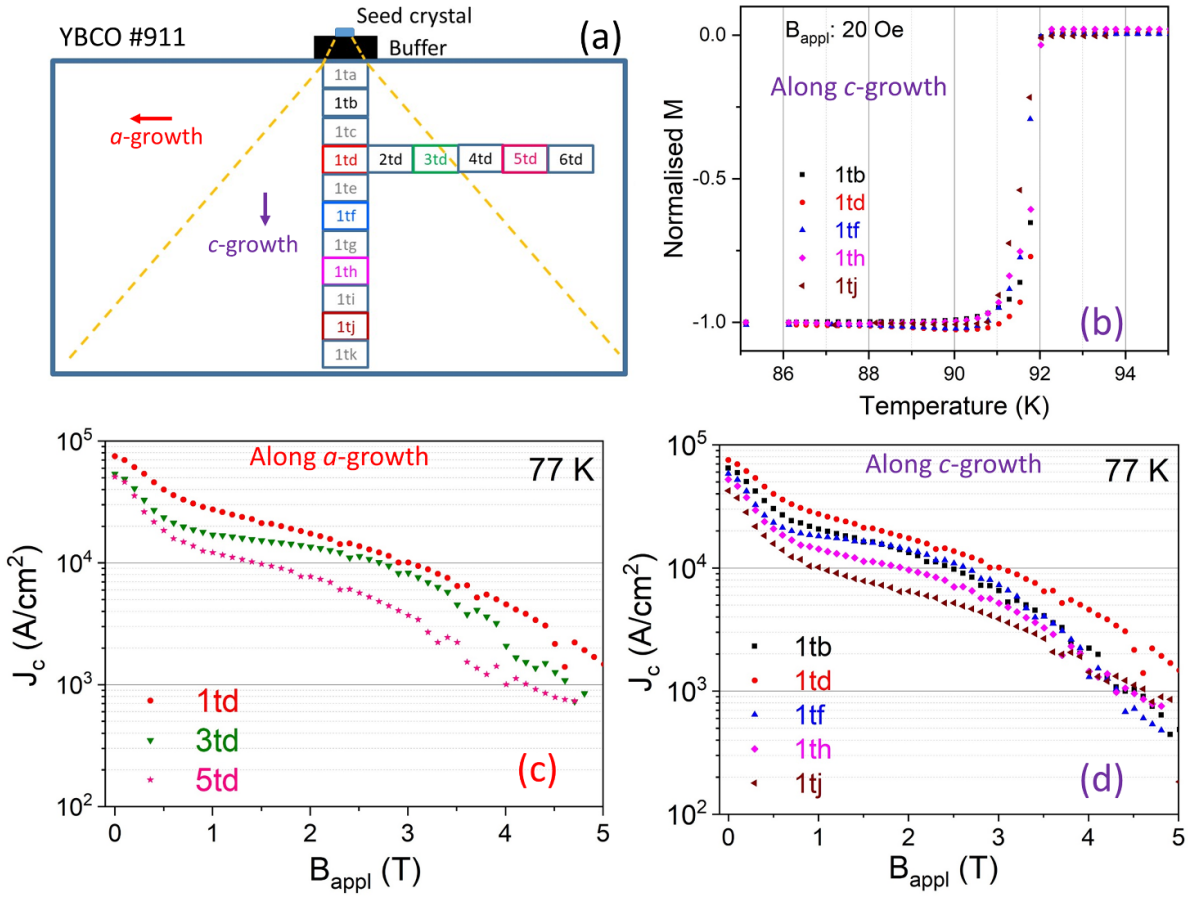

Figure 4. (a) Locations within the single grain YBCO sample fabricated by the 2-step BA-TSIG process (sample #911) where the sub-specimens were extracted for magnetisation measurements. (b) Normalised magnetisation (M) as a function of temperature showing the onset of critical temperature T_c for sub-specimens obtained from the c-growth region of the sample to be ~92 K. (c) and (d) Field dependence of the critical current density, $J_c(B)$, obtained within both the a- and c-growth regions of the sample, respectively.

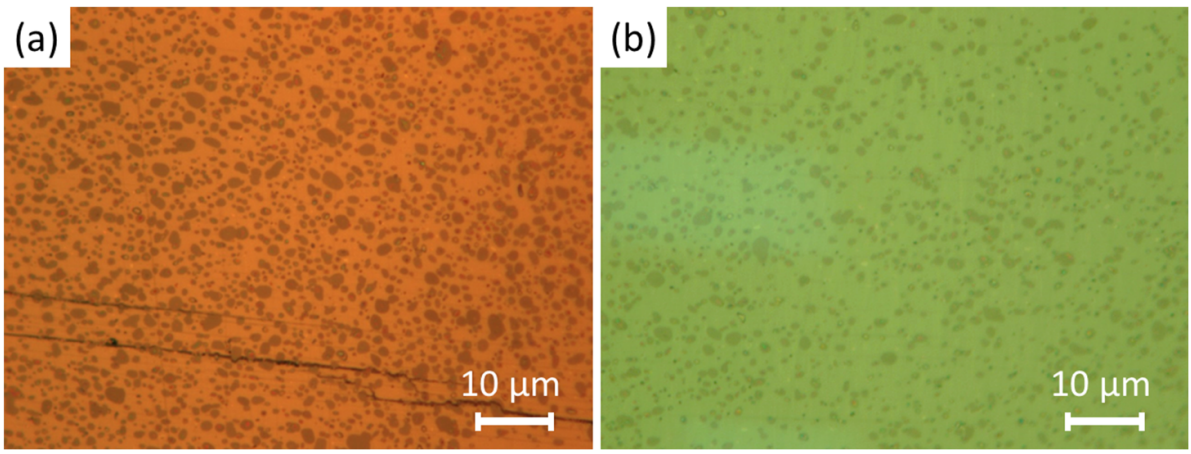

Figure 5. Optical micrographs obtained under a magnification of 1000x showing the presence of Y-211 inclusions in the Y-123 matrix for a single grain sample processed by (a) 1-step (#700) and (b) 2-step BA-TSIG (#911).

equilibrium. The trapped magnetic field was then measured using a rotating scanning system equipped with a linear array of 19 Hall probes. The three-dimensional trapped field profiles measured at 77 K at heights above the sample surface of 1.5 mm (#700) and 2 mm (#911) are shown in figure 2. The difference of 0.5 mm in the measurement heights was unavoidable due to an essential modification made to the setup to add a 0.5 mm protective Stycast™ layer to avoid damage to the Hall probes during their rotation in close proximity to the sample. This modification was made (in the period of several months) after full characterisation of the 1-step BA-TSIG sample and before the 2-step BA-TSIG sample was fabricated.

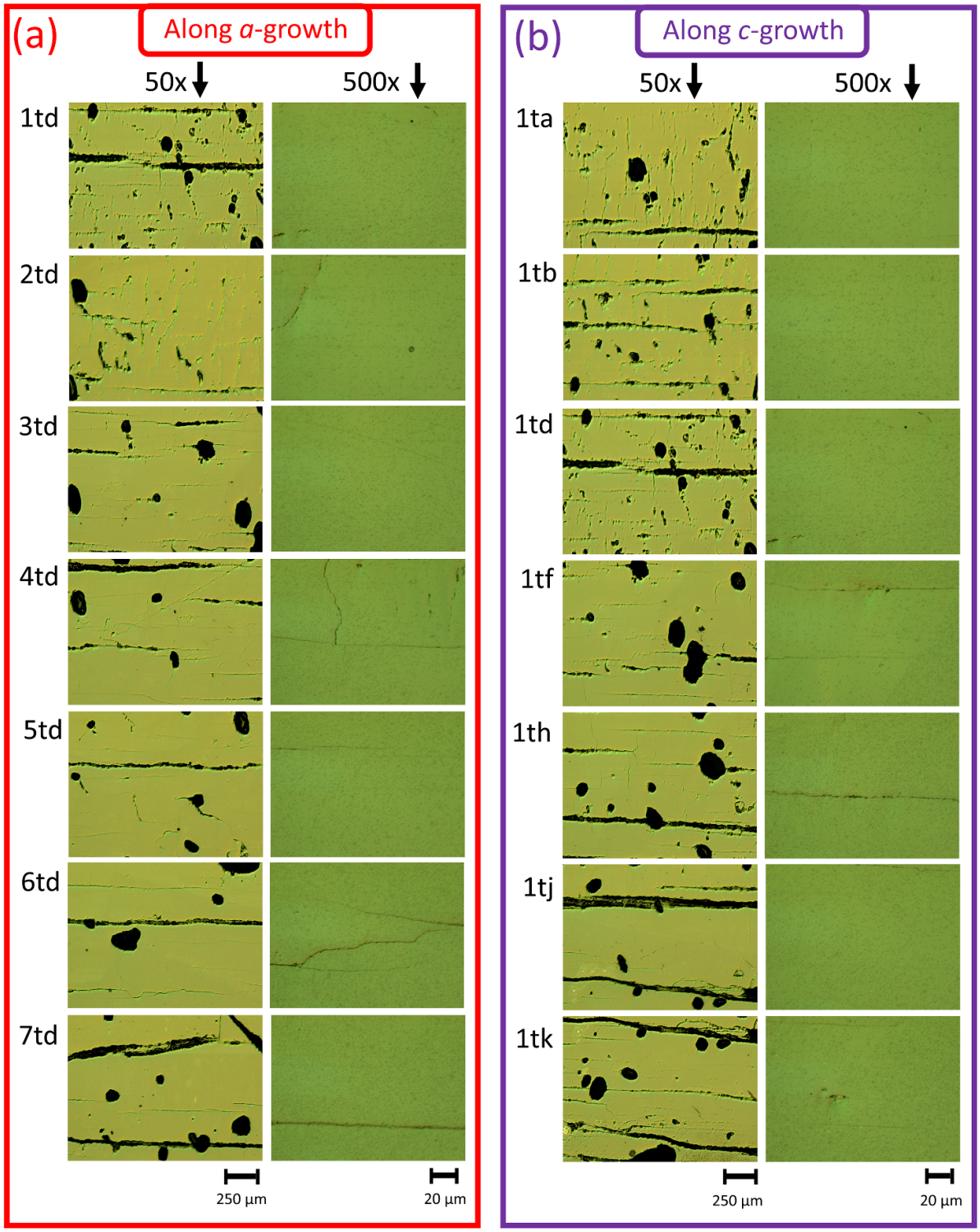

Figure 6. Optical micrographs obtained from the 2-step BA-TSIG processed YBCO sample (#911) under both low (50x) and high (500x) magnification, showing the porosity and Y-211 inclusions and their distribution within the Y-123 matrix. These features observed along the *a*-growth and *c*-growth regions of the sample are shown in (a) and (b), respectively. The labels indicate the same positions corresponding to those shown in figure 4(a).

The single peak observed in each of these measurements indicates that each sample constitutes a single grain. It can be seen that both samples exhibited a trapped field of ~0.86 T at 77 K at a height of 1.5–2 mm above the surface of the single grain.

2.3. Microstructure and critical current density

After the pulsed-field magnetisation experiments were completed (see section 3), the bulk samples were sliced using a rotary diamond saw for examination of their microstructures

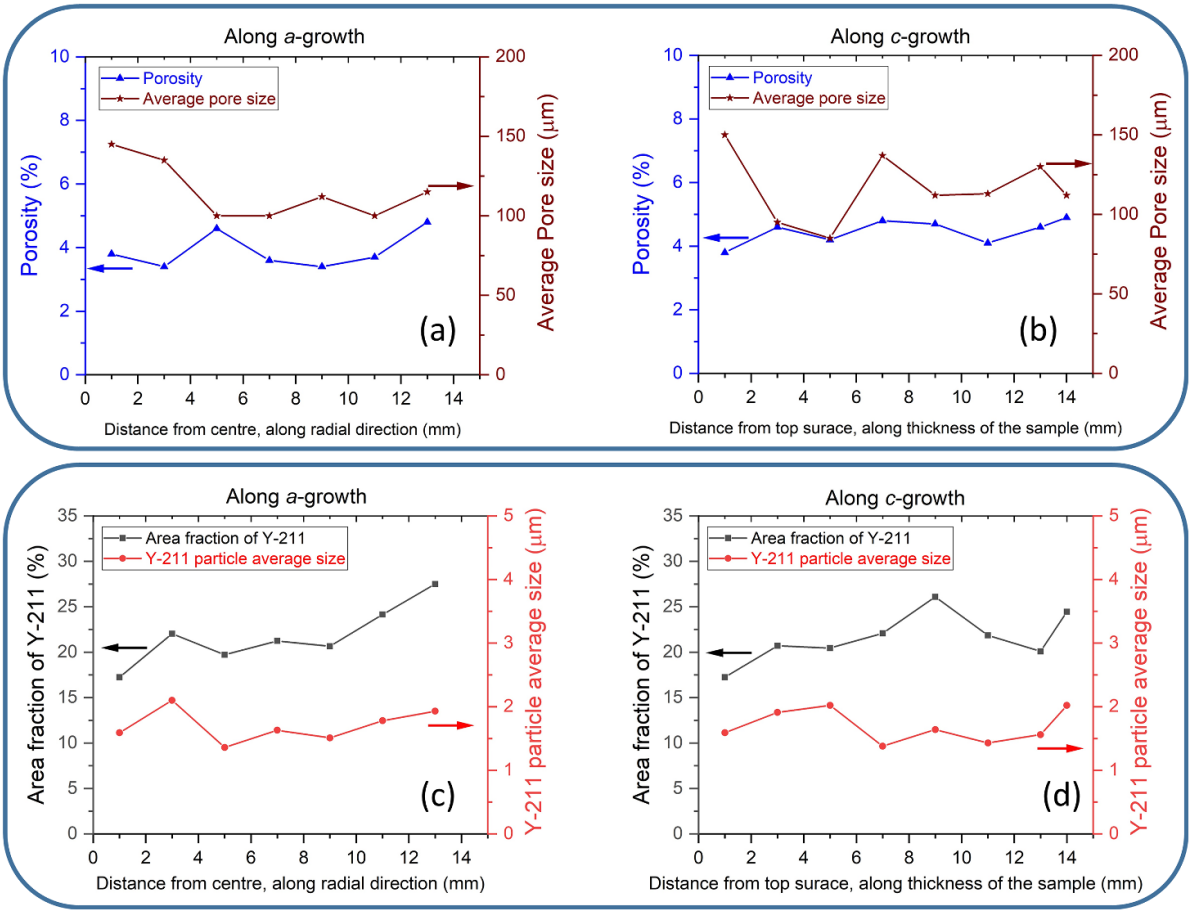

Figure 7. Quantitative analysis of the microstructural features of the 2-step BA-TSIG processed YBCO sample (#911). Variation of porosity and average pore-size analysed along the *a*-growth and *c*-growth regions of the sample are shown in (a) and (b), respectively. Y-211 area fraction and average size of Y-211 particles along both the *a*-growth and *c*-growth regions of the sample are shown in (c) and (d), respectively. Lines joining the data points are included as a guide for the eye.

and measurement of their local superconducting properties, including critical temperature T_c and $J_c(B)$. Sub-specimens were extracted from the centre of the parent single grain for magnetometry studies, as shown schematically in figure 3(a). Magnetisation as a function of applied field (*M-H*) was measured for the sub-specimens using a SQUID magnetometer (Quantum Design). The *M-H* loops were measured systematically over a temperature range 30–85 K to quantify the flux pinning strength. The in-field, temperature-dependent critical current density, $J_c(B, T)$, was then calculated from each *M-H* loop using the extended Bean critical state model [36], as shown in figures 3(b) and (c). It is clear that the overall superconducting performance of the 2-step BA-TSIG sample is superior to that of the 1-step BA-TSIG sample, in good agreement with previous studies [25, 27]. The 2-step BA-TSIG processing resulted in current densities $\geqslant$40 kA cm^{-2} in a field of 5 T at 65 K and $\geqslant$100 kA cm^{-2} in a field of 5 T in the temperature range: 30–50 K. The uniformity of the superconducting properties in the 2-step BA-TSIG processed YBCO sample was assessed by measuring $J_c(B)$ at 77 K for sub-specimens extracted from both the *a*-growth and *c*-growth regions of the sample, as shown in figure 4. A uniform T_c with onset ~92 K and a narrow superconducting transition width $\Delta T_c < 1$ K is observed in the samples, as shown in figure 4(b). It can be seen in figures 4(c) and (d) that the field dependence of critical current density at 77 K was nearly uniform with $J_c(0)$ ~ 50–60 kA cm^{-2} and specimens were found to maintain J_c of ~1 kA cm^{-2} even at 5 T external field. This unique uniformity in local superconducting properties is achieved through the advancement in the processing of (RE)BCO bulk superconducting materials.

The second half of each of the sliced single grains was polished sequentially with SiC paper and a colloidal suspension containing diamond particles down to the 1-micron level and observed under an optical microscope equipped with a polariser. The optical micrographs obtained under a magnification of 1000x revealing the presence of the Y-211 inclusions in the Y-123 phase matrix, obtained for the samples processed by 1-step and 2-step BA-TSIG, are shown in figures 5(a) and (b), respectively. These micrographs were analysed for Y-211 content using *ImageJ* software. The analysis showed that the 1-step BA-TSIG processing technique resulted in Y-211 particles with an average size of ~2.2 μm and comprising ~40% of the sample volume, whereas 2-step BA-TSIG processing reduced the average Y-211 particle size to ~1.5 μm with an associated volumetric content of ~24%, which is promising for achieving improved superconducting properties through optimised flux pinning. The control and

optimisation of Y-211 content in the Y-123 matrix has been known to enhance the critical current density via the creation of interfacial defects, which are known to aid significantly magnetic flux pinning.

A detailed microstructural study carried out on the 2-step BA-TSIG YBCO sample, along both the *a*-growth and *c*-growth regions, is presented in figure 6. Microstructural features, such as porosity and typical Y-211 size and distribution within the Y-123 matrix, can be seen from the optical micrographs recorded under both low (50x) and high (500x) magnification. These microstructural features were analysed quantitatively using *ImageJ* software, as shown in figure 7. It can be seen that the porosity is significantly smaller (<5 %) in comparison to the conventional TSMG-processed samples (where the porosity is ~15%), confirming the physically dense nature of the sample processed by infiltration growth. Furthermore, it can be observed from the optical micrographs that the Y-211 content is within the range of 18%–25% in the areas analysed. This relatively smaller variation in Y-211 secondary phase content is a key figure of merit for 2-step BA-TSIG processing, which leads to a more homogeneous microstructure and is the principal reason for observation of uniform superconducting properties [see figures 4(c) and (d)]. Analysis of the microstructure has clearly demonstrated a more homogeneous Y-211 distribution with an overall more optimum Y-211 content for the sample fabricated by the 2-step BA-TSIG technique, in addition to further refinement of these flux pinning sites. The combination of these characteristics of the sample has together produced a considerable improvement in both the superconducting performance of YBCO and in obtaining a uniform $J_c(B, T)$ across the sample volume. The results obtained for these samples with respect to $J_c(B, T)$ and microstructure are also in good agreement with those reported previously for the 2-step BA-TSIG processing technique [25, 27].

3. Pulsed-field magnetisation experiments

The machined and polished TSIG-processed YBCO samples for the PFM experiments were mounted tightly in non-magnetic 316-stainless steel ring-shaped sample holders using Stycast™, as shown in figure 8(a). The dimensions of these sample assemblies were as provided in table 1. The outer diameter of the stainless-steel sample holder was machined to 56 mm so that it matched the diameter of the PFM cold stage for effective and efficient cooling. Further details of the PFM facility employing the copper-wound solenoid coil can be found elsewhere [30], and only a brief description is provided here. A schematic illustration of the PFM assembly is shown in figure 8(b). The system comprises a Gifford-McMahon (GM) closed-cycle helium refrigerator and a copper-wound solenoid coil, 99 mm in inner diameter, 121 mm in outer diameter and 50 mm in height. This solenoidal magnetising coil is cooled using liquid nitrogen outside of the vacuum chamber used to contain the sample during magnetisation. The sample holder is fixed to the cold stage such that the applied field is parallel to the *c*-axis of the sample. Applied fields (B_{ex}) up to 6 T were applied to each sample, with a typical rise time of the excitation pulse of 13 ms and a duration of ~120 ms. After applying the pulsed field, the resultant trapped field in the sample was recorded after a 180 ms time delay, i.e. at $t = 300$ ms, using an axial-type Hall sensor on a controlled *x*-*y* stage. The magnitude of the pulsed field applied to each sample was calculated by measuring the current flowing through a shunt resistor in the circuit.

PFM experiments were carried out at temperatures of 65 K and 40 K with applied, pulsed magnetic fields up to 6 T. Figure 9 shows the trapped field (B_t) measured as a function of applied field (B_{ex}), obtained independently in both the samples. Similar PFM experiments were also carried out on a YBCO sample (#747; 29.5 mm diameter, 14.3 mm height) fabricated via the traditional TSMG approach to enable comparison between the two processing techniques (details of the TSMG sample used in this comparison can be found elsewhere [37]) and the results are included in figure 9 for reference. It should be noted that the measurement was carried out at the sample surface (0 mm) for the TSMG and 1-step BA-TSIG samples, whereas there was 1 mm separation between the surface of the sample and the Hall probe in the experiments carried out on the single grain fabricated by 2-step BA-TSIG (1 mm). The sample fabricated by 2-step BA-TSIG performed similarly to the other samples at 65 K, but clearly demonstrated superior performance at 40 K, trapping a maximum field of 2.19 T. It is to be noted that the trapped field measurements on the samples were carried out at different surface-Hall probe separations (0 mm in the 1-step BA-TSIG sample and + 1 mm in the 2-step BA-TSIG sample), which was unavoidable due to modifications made to the experimental arrangement between the sets of measurements (a more meaningful comparison between the samples is made later in figure 11), but this does not detract from the significance of the results of this investigation. Two-dimensional trapped field profiles measured at 2 mm/3 mm above the sample surfaces at both 65 K and 40 K are also shown in the figure. Trapped field as a function of time at 40 K, which represents a comparative performance of all the three samples, is shown in figure 10. The trapped fields measured in each of the samples at $t = 300$ ms, a temperature of 40 K and an applied field of 5 T are provided in the table in figure 10.

The time dependence of the measured magnetic field can assist in elucidating the trapped field improvement in the bulk superconductor fabricated by 2-step BA-TSIG. There are two conditions that should be considered in the PFM process to trap fields closer to the sample capability as indicated by FCM, i.e. $B_t \approx B_{ex}$:

- During the field ascending stage (i.e. below the peak of B_{ex}, which is achieved at $t = 13$ ms) B_{in} is equivalent to B_{ex}, and the flux penetration is homogeneous within the interior of the bulk single grain. In other words, B_t generated by PFM cannot exceed B_{in} during this stage of the magnetisation process. In this case B_t should be <3.60 T after PFM under the specified conditions for the sample fabricated by the 2-step BA-TSIG process.
- During the field descending stage (i.e. after 13 ms) there is no significant flux flow without heat generation, so as small

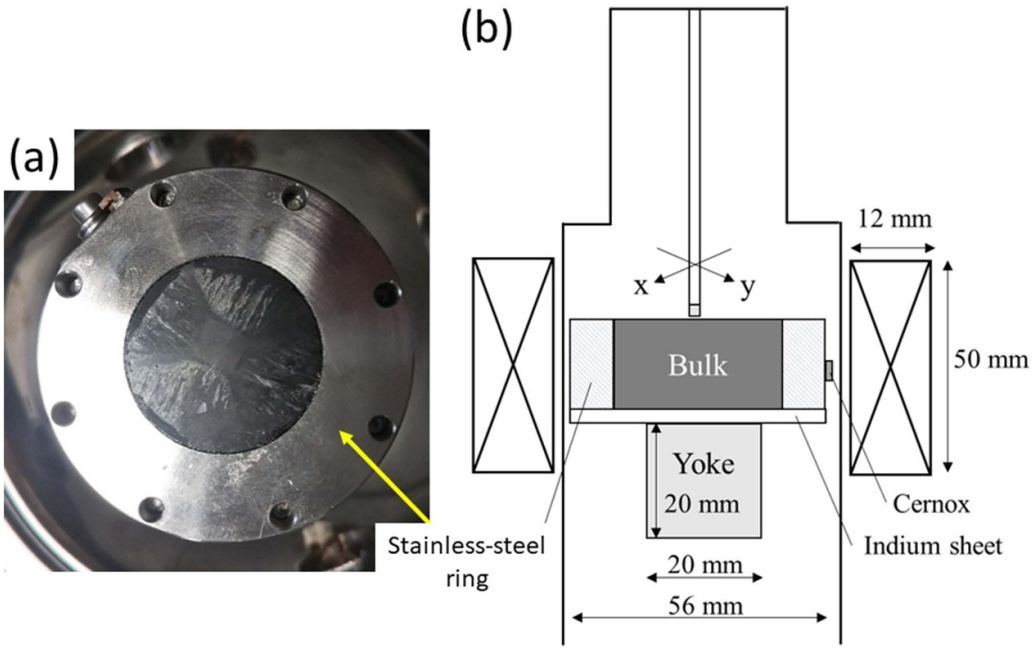

Figure 8. (a) A YBCO sample mounted tightly in 316-stainless steel using Stycast™. (b) Schematic illustration of the pulsed-field magnetisation system using a copper-wound solenoid coil. A cylindrical iron yoke (20 mm in diameter and 20 mm in height) is located underneath the sample.

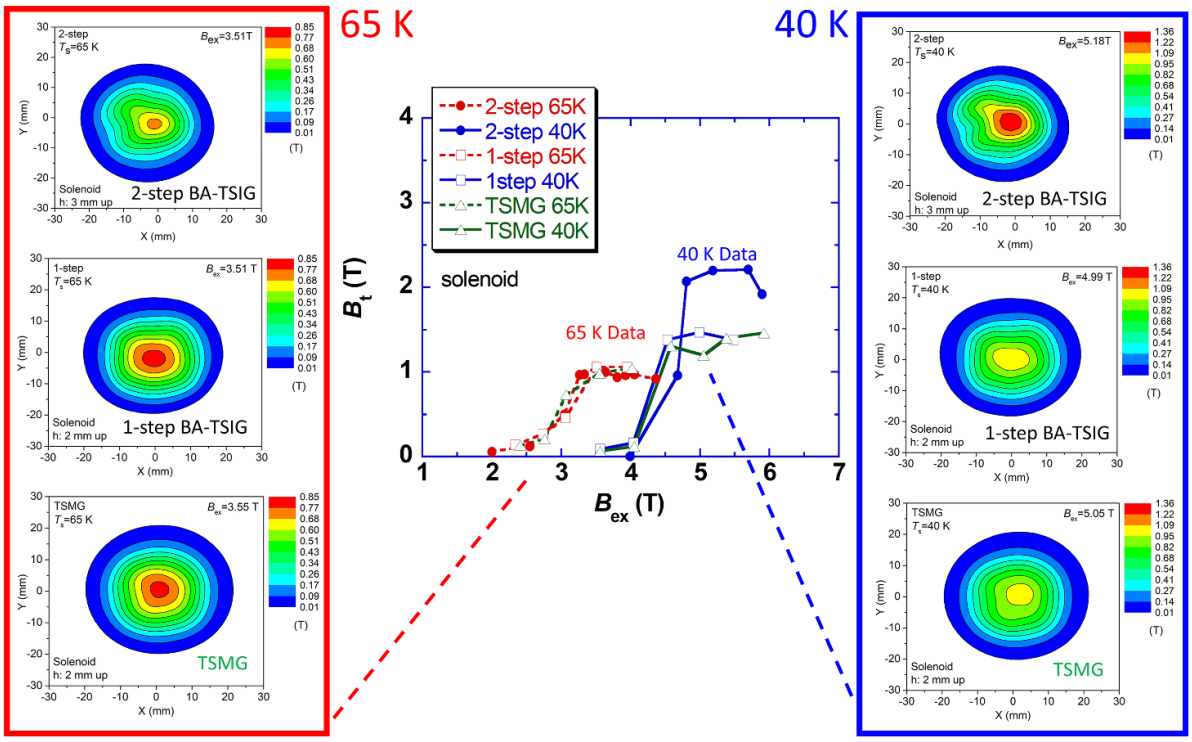

Figure 9. Trapped field (B_t) obtained via PFM experiments carried out at 65 K and 40 K for the TSIG-processed YBCO samples (1-step BA-TSIG #700 and 2-step BA-TSIG #911). For reference, similar experimental data obtained from a traditional TSMG-processed YBCO sample (#747) are also provided. It should be noted that the trapped field was measured at the sample surface for the TSMG and 1-step BA-TSIG samples, whereas the Hall sensor was positioned 1 mm away from the sample surface for the 2-step BA-TSIG sample. 2D trapped field profiles measured at 2 or 3 mm above the sample surface are also provided. Here, T_s is the sample temperature, B_{ex} is the applied field and h is the height above the sample at which the trapped field is measured.

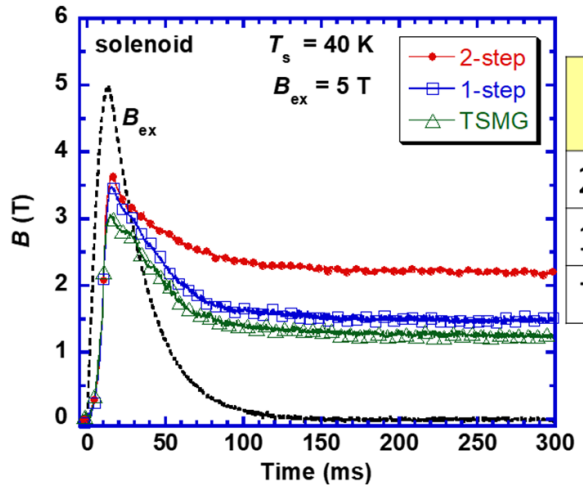

Bulk	B_{ex}	B_{in} @ 13 ms	B_t @ 300 ms
2-step	5.18 T	3.60 T	**2.19 T**
1-step	4.99 T	3.46 T	1.47 T
TSMG	5.05 T	3.03 T	1.22 T

Figure 10. Results from the PFM experiments carried out on the YBCO samples (2-step BA-TSIG, 1-step BA-TSIG and TSMG) at 40 K for an applied pulsed field of 5 T, which is close to the full magnetisation field (see figure 9). The applied pulsed field (curve in black color) and trapped magnetic field as a function of time are shown. The actual applied field 'B_{ex}', the induced field 'B_{in}' (the field measured at the peak of the pulse, i.e. $t = 13$ ms) and the trapped field 'B_t' (after the pulse, at $t = 300$ ms) are provided in the table.

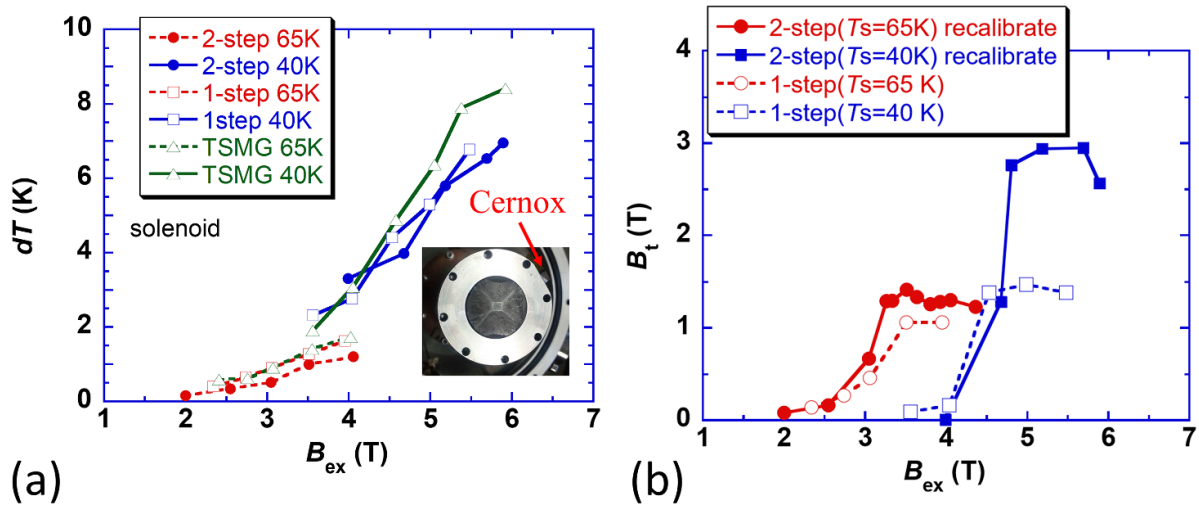

Figure 11. (a) Applied field (B_{ex})-dependence of the maximum temperature rise (dT) for the bulk YBCO samples (2-step BA-TSIG, 1-step BA-TSIG and TSMG) under investigation at 65 K and 40 K. The location of the Cernox temperature sensor mounted on the outer-side of the stainless steel ring and used to measure the temperature rise, dT is shown in the inset of the figure. (b) The recalibrated trapped fields for the 2-step BA-TSIG sample are provided in (b) to enable a meaningful comparison to be made. A trapped field as high as 3 T has been achieved at 40 K on the surface of the YBCO sample processed by the 2-step BA-TSIG technique.

a temperature rise as possible is desired, and the presence of the iron yoke below the bulk sample can assist in reduced flux dispersion within the x-y plane.

The reason for the improvement in trapped field illustrated in figure 10 is likely to be associated with the more homogeneous Y-211 distribution in the sample microstructure as observed in figures 6 and 7. This results in more homogeneous flux penetration and thereby reduces heat generation during PFM, which is evidenced in the maximum temperature rise, dT, shown in figure 11(a), measured by a Cernox temperature sensor mounted on the outer-side of the stainless steel ring. The sample processed by 2-step BA-TSIG exhibits the lowest temperature rise at both 65 K and 40 K. These results indicate that a specific approach focused on understanding the microstructural features of the sample could improve significantly the trapped field performance by PFM (i.e. a homogeneous distribution of Y-211 inclusions and subsequent uniform J_c properties, can result in more efficient pulsed-field magnetisation and the generation of higher trapped fields under the same magnetising conditions).

As mentioned earlier, the trapped fields shown in figure 9 were measured at different heights above the sample surface: 0 mm in the 1-step BA-TSIG sample and + 1 mm in the 2-step BA-TSIG sample. To enable a fair comparison, the trapped fields for the 2-step BA-TSIG sample are recalculated using equation (1), based on the Biot–Savart law, to estimate their value at the surface of the single grain [38].

$$B_t(z) = \frac{\mu_0 J_c}{2}\left[(z+t)\ log\left(\frac{\frac{D}{2}+\sqrt{\left(\frac{D}{2}\right)^2+(z+t)^2}}{z+t}\right) - z\ log\left(\frac{\frac{D}{2}+\sqrt{\left(\frac{D}{2}\right)^2+z^2}}{z}\right)\right]. \quad (1)$$

z is the distance above the centre of the top surface of the sample, and D and t are the diameter and thickness of the disc-shaped bulk superconductor.

As a result, a more meaningful comparison of the values of trapped field is provided in figure 11(b). It is promising to observe in the present study that a surface trapped field of ~3 T has been achieved in a basic YBCO sample processed by infiltration growth processing via a relatively simple single-pulse magnetisation process using a copper-wound solenoid coil. This value of trapped field is comparable with, or superior to, the results of many previous PFM studies on YBCO and GdBCO bulk single grains of similar dimensions and at similar temperatures [37–42]. There is, of course, further scope to improve this performance either via multi-pulse magnetisation with step-wise cooling and/or through the use of a split coil magnetisation geometry. The fact that higher pulsed-field magnetisation efficiency is achievable by employing (RE)BCO bulk single grains with greater homogeneity is greatly encouraging from an applications perspective.

4. Conclusion

Pulsed-field magnetisation using a copper-wound solenoid has been used to investigate the magnetic field trapping properties of bulk, single grain YBCO superconductors fabricated by TSIG process at 65 K and 40 K. The YBCO sample fabricated by the 2-step buffer-assisted TSIG technique trapped a significantly larger magnetic field from a single pulse magnetisation process (~3 T at 40 K) than is obtained typically in traditional melt grown samples. This improvement is attributed to the lower temperature rise in samples fabricated by TSIG during pulsed-field magnetisation due to the more homogeneous microstructure and uniform superconducting properties of these samples. This observation suggests that the use of a 2-step BA-TSIG process for the fabrication of (RE)BCO systems both with and without added Ag could lead to a substantial improvement in pulsed-field magnetisation performance and to more competitive engineering applications.

Acknowledgments

This research was supported by the following projects: JSPS KAKENHI Grant No. 15K04646; King Abdualaziz City for Science and Technology (KACST); and the Engineering and Physical Sciences Research Council (EPSRC) with grant code: EP/P00962X/1. M D Ainslie would like to acknowledge financial support from an EPSRC Early Career Fellowship, EP/P020313/1. Data supporting this publication are available at the University of Cambridge data repository https://doi.org/10.17863/CAM.53945

ORCID iDs

Devendra K Namburi https://orcid.org/0000-0003-3219-2708
K Takahashi https://orcid.org/0000-0002-8278-2688
T Hirano https://orcid.org/0000-0003-1658-914X
H Fujishiro https://orcid.org/0000-0003-1483-835X
Y-H Shi https://orcid.org/0000-0003-4240-5543
D A Cardwell https://orcid.org/0000-0002-2020-2131
J H Durrell https://orcid.org/0000-0003-0712-3102
M D Ainslie https://orcid.org/0000-0003-0466-3680

References

[1] Durrell J H, Ainslie M D, Zhou D, Vanderbemden P, Bradshaw T, Speller S, Filipenko M and Cardwell D A 2018 Bulk superconductors: a roadmap to applications *Supercond. Sci. Technol.* **31** 103501
[2] Murakami M 2007 Processing and applications of bulk RE-Ba-Cu-O superconductors *Int. J. Appl. Ceram. Technol.* **4** 225–41
[3] Larbalestier D, Gurevich A, Feldmann D M and Polyanskii A 2001 High T_c superconducting materials for electric power applications *Nature* **414** 368–77
[4] Li B, Zhou D, Xu K, Hara S, Tsuzuki K, Miki M, Felder B, Deng Z and Izumi M 2012 Materials process and applications of single grain (RE)–Ba–Cu–O bulk high-temperature superconductors *Phys.* C **482** 50–57
[5] Namburi D K, Durrell J H, Jaroszynski J, Shi Y-H, Ainslie M D, Huang K, Dennis A R, Hellstrom E E and Cardwell D A 2018 A trapped field of 14.3 T in Y–Ba–Cu–O bulk superconductors fabricated by buffer-assisted seeded infiltration and growth *Supercond. Sci. Technol.* **31** 125004
[6] Krabbes G, Fuchs G, Verges P, Diko P, Stover G and Gruss S 2002 16 T trapped field in modified YBaCuO: materials aspects *Phys.* C **378-381** 636–40
[7] Tomita M and Murakami M 2003 High-temperature superconductor bulk magnets that can trap magnetic fields of over 17 tesla at 29 K *Nature* **421** 517–20
[8] Durrell J H, Dennis A R, Jaroszynski J, Ainslie M D, Palmer K G B, Shi Y-H and Cardwell D A 2014 A trapped field of 17.6 T in melt-processed, bulk Gd-Ba-Cu-O reinforced with shrink-fit steel *Supercond. Sci. Technol.* **27** 082001
[9] Ren Y, Weinstein R, Liu J, Sawh R P and Foster C 1995 Damage caused by magnetic pressure at high trapped field in quasi-permanent magnets composed of melt-textured Y-Ba-Cu-O superconductor *Phys.* C **251** 15–26
[10] Nariki S, Sakai N and Murakami M 2005 Melt-processed Gd-Ba-Cu-O superconductor with trapped field of 3 T at 77 K *Supercond. Sci. Technol.* **18** S126–30
[11] Shiohara Y and Endo A 1997 Crystal growth of bulk high-Tc superconducting oxide materials *Mat. Sci. Eng.* **R19** 1–86
[12] Salama K, Selvamanickam V, Gao L and Sun K 1989 High current density in bulk $YBa_2Cu_3O_x$ superconductor *Appl. Phys. Lett.* **54** 2352
[13] Sudhakar Reddy E and Rajasekharan T 1998 Fabrication of textured $REBa_2Cu_3O_{7-\delta}$ RE_2BaCuO_5 (RE = Y, Gd) composites by infiltration and growth of RE_2BaCuO_5 preforms by liquid phases *Supercond. Sci. Technol.* **11** 523–34
[14] Yang P, Yang W, Zhang L, Chen L and Wang M 2019 Bottom-seeded infiltration and growth for fabrication of single-grain GdBCO superconducting ring *IEEE Trans. Appl. Supercond.* **29** 6802705

[15] Chow J C L, Leung H T, Lo W and Cardwell D A 1998 Analysis of the spatial distribution of Y_2BaCuO_5 inclusions in large-grain $YBa_2Cu_3O_{7-\delta}$ *J. Mater. Sci.* **33** 1083–9

[16] Chen Y L, Chan H M, Harmer M P, Todt V R, Sengupta S and Shi D 1994 A new method for net-shape forming of large, single-domain $YBa_2Cu_3O_{6+x}$ *Phys.* C **234** 232–6

[17] Kim C J, Jee Y A, Lee K W, Sung T H, Han S C, Kuk I H and Hong G W 1998 Low temperature melt process of $SmBa_2Cu_3O_{7-y}$ using a liquid infiltration technique *Appl. Supercond.* **6** 149–56

[18] Viswanath N V N, Rajasekharan T, Harish Kumar N, Menon L and Malik S K 1998 Infiltration growth processing of $SmBa_2Cu_3O_y$ superconductor *Supercond. Sci. Technol.* **11** 420

[19] Cloots R, Koutzarova T, Mathieu J-P and Ausloos M 2005 From RE-211 to RE-123. how to control the final microstructure of superconducting single-domains *Supercond. Sci. Technol.* **18** R9

[20] Naik S P K and Seshubai V 2017 Role of nano and micron-sized inclusions of the oxygen controlled preform optimized infiltration growth processed YBCO superconductors *J. Phys. Chem. Solids* **101** 65–73

[21] Das D, Muralidhar M, Ramachandra Rao M S and Murakami M 2017 Top-seeded infiltration growth of (Y, Gd)$Ba_2Cu_3O_y$ bulk superconductors with high critical current densities *Supercond. Sci. Technol.* **30** 105015

[22] Diko P, Vojtkova L, Vojtko M and Rajnak M 2018 Microstructural aspects of infiltration growth YBCO bulks with chemical pinning *IEEE Trans. Appl. Supercond.* **29** 6800805

[23] Namburi D K, Shi Y, Palmer K G, Dennis A R, Durrell J H and Cardwell D A 2016 An improved top seeded infiltration growth method for the fabrication of Y–Ba–Cu–O bulk superconductors *J. Eur.Ceram. Soc.* **36:** 615–24

[24] Wang M, Yang P-T, Yang W-M, Li J-W and Hassan Q U 2015 The fabrication process of a high performance and pure c-axis grown GdBCO bulk superconductor with the TSMT-IG technique *Supercond. Sci. Technol.* **28** 105011

[25] Namburi D K, Shi Y, Palmer K G, Dennis A R, Durrell J H and Cardwell D A 2016 Control of Y-211 content in bulk YBCO superconductors fabricated by a buffer-aided, top seeded infiltration and growth melt process *Supercond. Sci. Technol.* **29** 034007

[26] Wang W M, Chen L P and Wang X J 2015 A new RE + 011 TSIG method for the fabrication of high quality and large size single domain YBCO bulk superconductors *Supercond. Sci. Technol.* **29** 024004

[27] Namburi D K, Shi Y, Palmer K G, Dennis A R, Durrell J H and Cardwell D A 2016 A novel, two-step top seeded infiltration and growth process for the fabrication of single grain, bulk (RE)BCO superconductors *Supercond. Sci. Technol.* **29** 095010

[28] Ainslie M D and Fujishiro H 2015 Modelling of bulk superconductor magnetisation *Supercond. Sci. Technol.* **28** 053002

[29] Fujishiro H, Tateiwa T, Fujiwara A, Oka T and Hayashi H 2006 Higher trapped field over 5 T on HTSC bulk by modified pulse field magnetising *Phys.* C **445–48** 334–8

[30] Ainslie M D, Fujishiro H, Ujiie T, Zou J, Dennis A R, Shi Y-H and Cardwell D A 2014 Modelling and comparison of trapped fields in (RE)BCO bulk superconductors for activation using pulsed field magnetisation *Supercond. Sci. Technol.* **27** 065008

[31] Deng Z, Shinohara N, Miki M, Felder B, Tsuzuki K, Watasaki M, Kawabe S, Taguchi R and Izumi M 2012 Pulsed-field magnetization properties of bulk superconductors by employment of vortex-type coils *Phys. Procedia* **36** 958–62

[32] Zhou D, Ainslie M D, Srpcic J, Huang K, Shi Y-H, Dennis A R, Cardwell D A, Durrell J H, Boll M and Filipenko M 2018 Exploiting flux jumps for pulsed field magnetisation *Supercond. Sci. Technol.* **31** 105005

[33] Yang W M, Li G Z, Chao X X, Li G W, Guo F X, Chen S L and Ma J 2011 Fabrication of single domain GdBCO bulks with different new kind of liquid sources by TSIG technique *Phys.* C **471** 850–3

[34] Li G-Z and Yang W-M 2010 Fabrication and superconducting property of large single-domain Gd–Ba–Cu–O bulk using Yb-based liquid source *J. Supercond. Novel Mag.* **23** 429–32

[35] Namburi D K, Shi Y-H, Zhai W, Dennis A R, Durrell J H and Cardwell D A 2015 Buffer pellets for high-yield, top-seeded melt growth of large grain Y-Ba-Cu-o superconductors *Cryst. Growth. Des.* **15** 1472–80

[36] Gyorgy E M, van Dover R B, Jackson K A, Schneemeyer L F and Waszczak J V 1989 Anisotropic critical currents in $Ba_2YCu_3O_7$ analyzed using an extended Bean model *Appl. Phys. Lett.* **55** 283

[37] Takahashi K, Ainslie M D, Fujishiro H, Naito T, Shi Y-H and Cardwell D A 2017 Trapped field properties of a Y–Ba–Cu–O bulk by pulsed field magnetization using a split coil inserted by iron yokes with various geometries and electromagnetic properties *Phys.* C **536** 1–10

[38] Naito T, Sasaki T and Fujishiro H 2012 Trapped magnetic field and vortex pinning properties of MgB_2 superconducting bulk fabricated by a capsule method *Supercond. Sci. Technol.* **25** 095012

[39] Ohsaki H, Shimosaki T and Nozawa N 2002 Pulse field magnetization of a ring-shaped bulk superconductor Supercond *Sci. Technol.* **15** 754–8

[40] Shiraishi R, Fujiyama K and Ohsaki H 2005 Macroscopic magnetic flux motion in Y-Ba-Cu-O bulk superconductor during pulsed field magnetization *IEEE Trans. Appl. Supercond.* **15** 3153–6

[41] Yokoyama K and Oka T 2020 Influence of the shape of soft-Iron yoke on trapped field performance of HTS bulk *IEEE Trans. Appl. Supercond.* **30** 6800105

[42] Yanagi Y, Itoh Y, Yoshikawa M, Oka T, Ikuta H and Mizutani U 2005 Pulsed field magnetisation of a 36 mm diameter single-domain Sm-Ba-Cu-O bulk superconductor at 30, 35 and 77 K *Supercond. Sci. Technol.* **18** 839